Pergamon

0301-9322(94)00045-X

ANALYTICAL CALCULATION OF DNB-SUPERHEATING BY A POSTULATED THERMO-MECHANICAL EFFECT OF NUCLEATE BOILING†

D. SCHROEDER-RICHTER and G. BARTSCH

Technical University of Berlin, Institute of Energy Engineering, Marchstraße 18,
D-10587 Berlin, Germany

Abstract—Observations of stationary subcooled nucleate boiling with forced convection in a glass-pipe at a pressure of 0.1 MPa lead to a new interpretation of the superheated liquid state wetting the heated wall. This interpretation applied to the rules of linear non-equilibrium thermodynamics results in framework equations with non-linear heat transfer as indicated by several empirical correlations. Momentum balances at the singular surfaces of a bubble have been combined with a sonic limit for the mass transfer through the interfaces serving as a maximum condition with respect to heat transfer (DNB). The calculation predicts the corresponding wall temperature from properties of state without using empirical coefficients and therefore must be valid independent of coolants' geometries and surface conditions. Documented measurements at pool boiling, forced and free convection with cryogenic liquids, water and liquid metals emphasize this if data are properly selected corresponding to the precondition that void fraction remains low.

Key Words: nucleate boiling, thermodynamics of irreversible processes, superheated liquid, thermo-mechanical effect, departure from nucleate boiling (DNB), cryogenic liquids, water, liquid metals

1. INTRODUCTION

Flow boiling has been investigated for more than forty years and has been mainly supported by special interest in chemical processing and energy engineering. In particular, nuclear energy has enabled the submission of arbitrary heat fluxes to a channel with boiling flow. Economic interest in generating maximum electrical power with compact heat exchangers presents a new problem. It has been observed that the heat transfer surface suddenly dries out when a maximum heat flux is to be transferred. The vapour covering the heat transfer surface then hinders the heated wall to be cooled by the flowing liquid and thus the temperature rises rapidly and may destroy the flow channel. For this reason, special knowledge about these boiling phenomena is required in order to minimize the risk of such accidents.

Numerous correlations have been obtained over the last few decades to predict the heat flux transferred during flow boiling as well as the maximum heat flux (i.e. the so-called critical heat flux, CHF). Various improvements to the boiling correlations have been thoroughly checked by Celata *et al.* (1986) and Hahne *et al.* (1989). Critical heat flux has been studied recently by Weber (1990) using excellent experimental facilities. All these empirical results show arbitrary complexity dependent on selected, previously investigated flow parameters. Analytical results obtained without using empirical coefficients are very scarce, e.g. Zuber (1958) predicting critical heat flux during pool boiling on a horizontal plate, Spiegler *et al.* (1963) predicting the wall temperature during minimum heat flux (i.e. when the heat transfer surface is just completely dry) and Hewitt & Hall-Taylor (1970) predicting the dry-out limit from a balance of liquid mass wetting the heat transfer surface during annular flow.

Two idealized flow characteristics can be distinguished during boiling however. At low void fraction single bubbles appear surrounded by a continuous liquid phase flowing through the channel which is called nucleate boiling. With maximum heat flux the bubbles start to accumulate

---

†This study deals with a single aspect of the Ph.D. thesis by Schroeder-Richter (1991).

at the heated wall. This situation is called departure from nucleate boiling (DNB) and leads to inverted annular flow with a thin film of vapour covering the heated wall while the centre of the flow channel is still filled with liquid.

If the void fraction increases, the opposite occurs and the bubbles accumulate in the centre of the flow channel. In this case, the heated wall is covered with a thin film of liquid while the flow channel is filled with vapour (annular flow), which may carry some droplets of liquid. At maximum heat flux the liquid film dries out, i.e. its mass flow along the channel approaches zero (Hewitt & Hall-Taylor 1970).

At intermediate void fraction, the two flow patterns do not change distinctly but show some overlapping characteristics such as slug flow, churn flow, wispy-annular flow, etc. However, the present study does not try to describe the heat transfer characteristics corresponding to all of the possible flow regimes. Restrictions are still necessary to reduce the number of relevant parameters so that they become surveyable using analytical tools.

Recent literature (e.g. Groeneveld & Snoek 1986) has indicated that boiling phenomena show minor dependences on flow parameters during fully developed nucleate flow boiling. These results might justify the development of an idealized analytical model which can be applied at low void fraction (i.e. bubbly) flow boiling.†

As a very long period spent investigating the phenomena of flow boiling has led to only a few analytical results, it seems reasonable to consider some basic assumptions, which might be wrong even though they are generally accepted. We concluded the strong influence of apparent flow characteristics on boiling heat transfer and thus it is obvious that some hydrodynamics should be recalled.

From hydrodynamics we know that during laminar single-phase flow with rotational symmetry, constant pressure can be assumed over the cross section since secondary flow phenomena will not occur. In contrast, two-phase flow is mainly characterized by the occurrence of distinct secondary flow. A considerable momentum transfer can be caused by phase transitions which are due to the differences of both liquid and vapour densities. Hung (1979) has shown from the laws of non-equilibrium thermodynamics, that a corresponding pressure difference has to be taken into account for model development.

Despite this fact, constant pressure is usually assumed, since this mechanical non-equilibrium has not yet been detected by measurement. Using direct methods of pressure measurement, phase transition is completely hampered by the measuring instrument exactly at the position where the measurement is to be performed. On the other hand, the unknown pressure is not a parameter of hydrodynamics alone, but is also a property of the thermodynamic state. It is clear that the validity of any boiling model hinges on assumptions about which thermodynamic properties might prevail in vapour and liquid. Since the pressures are not measured (i.e. neither non-equilibrium nor equilibrium is verified) any of the assumptions are reasonable as the results of the models indicate proper predictions.

2. BASIC STEPS IN THE DEVELOPMENT OF A NEW MODEL

The present model is based on a new hypothesis for the thermodynamic state of the liquid wall layer near the heated surface. The new description of state is developed according to some observations during bubbly flow boiling. With that information we deduce a phenomenological law for heat transfer during fully developed nucleate flow boiling (i.e. bubbly flow) which is based on the thermodynamics of irreversible processes. This is not done to create a new correlation for boiling heat transfer, but to further emphasize the basic assumption about the thermodynamic state of the liquid wall layer. Finally we use the balance of momentum for a single bubble and some additional assumptions to conclude analytically that DNB occurs at a special property of state for the liquid wall layer, which can be solved for the temperature of the heated wall.

For verification we simply show that the framework of the new phenomenological law reconstructs empirical correlations and that it could be combined with the model predicting the

---

†This bubbly situation alone is called nucleate boiling in the following.

wall temperature at DNB when the critical heat flux is to be calculated. More work could be done to correlate the heat fluxes but the purpose of this study is to demonstrate the direct consequences of assuming a pressure excess in the liquid wall layer which is a fundamentally new hypothesis and thus shall be considered in detail here. This is performed when the analytical DNB prediction (without empirical coefficients) is verified using documented measurements for various fluids from cryogens up to liquid metals.

First we summarize some macroscopic aspects of the linear thermodynamics of irreversible processes which emphasize the analytical structure of phenomenological laws in contrast to empirical correlations assuming power laws without physical argument, except that the underlying law must eliminate all dimensions.

2.1. Some basic aspects to correlate irreversible processes

A typical discontinuous model (lumped body model) can be created when separating a thermodynamic system into several sub-systems which are assumed to be at thermodynamic equilibrium themselves. Thus, irreversible generation of entropy is possible only by exchange of quantities, e.g. mass, energy (which are called thermodynamic fluxes J_i, $i = 1, \ldots, n$), across the boundaries of the sub-systems. If we calculate the production of entropy for the total of all sub-systems

$$\Omega = \sum_{i=1}^{n} J_i X_i \geqslant 0,$$ [1]

we see that the fluxes contribute as linear combinations to the entropy generation, Ω. The weighting coefficients X_i are not arbitrary but result from the balance of entropy. They represent the differences of some thermodynamic potentials between the sub-systems and are usually called driving forces. Basic assumptions in the thermodynamics of irreversible process are, that all of the fluxes can be understood to be unknown functions of all driving forces

$$J_i = f_i(X_1, \ldots, X_n)$$ [2]

but these functions are assumed to be continuous around $X_k = 0$ ($k = 1, \ldots, n$) and to all have partial derivatives with respect to X_k (i.e. continuous fields are only assumed). The driving forces X_k are assumed to be small ($X_k \ll 1$).†

Taylor approximations of the functions f_i can then be developed

$$J_i = f_i(0, \ldots, 0) + \sum_{k=1}^{n} \left(\frac{\partial f_i}{\partial X_k}\right)_{X_1,\ldots,X_n = 0} X_k + \cdots,$$ [3]

where the terms of higher order show the powers of the small driving forces which can be ignored with respect to the first order terms. Additionally all fluxes J_i disappear at thermal equilibrium, i.e.

$$f_i(0, \ldots, 0) = 0.$$ [4]

The partial derivatives

$$L_{ik} = \frac{\partial f_i}{\partial X_k}$$ [5]

are usually named phenomenological coefficients. According to the Taylor series [3] they are independent of fluxes J_i and forces X_k. From [3], [4] and [5] we have the phenomenological law

$$J_i = \sum_{k=1}^{n} L_{ik} X_k,$$ [6]

---

†This assumption holds with very few exceptions for all engineering applications, e.g. X_k may be the difference between temperatures related to absolute temperature and is small for conduction heat transfer but large for radiation heat transfer.

which explicitly shows the dependence of fluxes J_i on all forces X_k. However, the thermodynamics of irreversible processes does not determine the phenomenological coefficients, which may depend on anything else other than fluxes and forces. Some restrictions are known but they are not of relevance here. The interested reader will find them in textbooks on thermodynamics.

All of the phenomenological coefficients that still remain unknown may, of course, be correlated using Buckingham's Π-theorem (which is not carried out here), but the development to [6] shows slightly more information than could be found using the dimensional analysis directly, e.g. the fluxes are expressed as linear combinations by [6] which are not arbitrary as with the products with powers of the dimensionless groups from the classical Buckingham method. Thus [6] can serve as an analytical framework for predicting heat transfer relations. The dependence of heat flux on wall superheating can be solved explicitly.

Before applying [1] to entropy production during nucleate flow boiling however, it is necessary to analyse the thermodynamic sub-systems and to describe the properties of state for each of them. A new hypothesis for the superheated wall layer is based on some observations.

3. OBSERVATION AND INTERPRETATION OF NUCLEATE BOILING

Investigations of Michel (1984) and Jansen (1988) dealt with stationary sub-cooled nucleate boiling with forced convection of water flowing at atmospheric pressure through an annulus which consists of a heating rod inserted concentrically into a glass-pipe. A high speed camera has been used for observation and documentation. It has been observed that:

(1) vapor bubbles move with considerable radial velocity from the heating rod into the subcooled liquid and
(2) the whole surface of the heating rod is wetted during nucleate boiling. A liquid microlayer is located even under the base of each bubble.

Our conclusions are:

(1) The radial velocity of the bubble is induced by the pressure p_w at the heated surface, which is higher than the bulk pressure p_b in the centre of the flow:

$$p_w > p_b. \tag{7}$$

(2) The recent assumption of constant pressure over the cross section rules out a new problem: "The temperature of the wetting liquid should be identical to the wall temperature of the heating rod which lies above the saturation temperature corresponding to p_b and should therefore describe a vapour state". A metastable thermodynamic sub-system is usually proposed to explain the liquid wall layer (Spiegler et al. 1963). However, upon inspecting the classical literature by the discoverers of metastable states (Berthelot 1850; Meyer 1911), we find the observation that metastable liquids are converted immediately into stable equilibria of vapour and liquid if small fluctuations of pressure occurred. In fact, considerable turbulence occurs during the boiling process and we can therefore summarize that a metastable sub-system cannot survive at steady-state conditions. Consequently, we replace the assumption of a metastable state by postulating a mechanical non-equilibrium in the sense of [7]. Wetting of the heating surface is only possible if the surface tempeature T_w is smaller than or equal to the saturation temperature T_s, which is determined by p_w

$$T_w \leqslant T_s(p_w). \tag{8}$$

To define a liquid state a considerable† mechanical non-equilibrium [7] will correspond to [8]. The equation of state combined with the equation of Clausius–Clapeyron specify for an ideal gas:

$$p_w \geqslant p_b \exp\left\{\frac{h_{LG}M}{R}\left[\frac{1}{T_s(p_b)} - \frac{1}{T_w}\right]\right\}, \qquad [9]$$

where h_{LG} is the enthalpy of evaporation, M is the molar mass and R is the ideal gas constant.

Boiling occurs close to the microlayer at the base of the bubbles. Therefore the thermodynamic state of the microlayer has to be close to the line of liquid saturation within the diagram of state. Then inequalities [8] and [9] can be transformed into equations. Zuber (1958) and Chen (1963) even made use of such a pressure difference to correlate boiling heat transfer but it has not been analysed in the present sense.

3.1. Pressure excess from the background of non-equilibrium thermodynamics

In the case of a small thermal non-equilibrium, heat will be transferred by convection only, i.e. entropy production $J_1 X_1$ consists of heat flux times temperature excess alone. In the case of intense heating with increasing heat flux, other heat transfer mechanisms (e.g. mass flux of evaporation associated with pressure excess) become more important. The growing influence of mechanical non-equilibrium (boiling) decreases the total entropy production $\Sigma J_i X_i$ by a reduction in the thermal non-equilibrium X_1 (at a given total heat flux and thus reduced convection heat flux J_1). On the other hand, the elevated pressure at the heated wall will tend to minimize the evaporation (by elevating the saturation temperature) in agreement with the moderation theorem by Braun (1887) and Le Chatelier (1888). Using the modern approach we could argue that the total entropy production $\Sigma J_i X_i$ reaches a minimum if the pressure excess [9] is not elevated above the value which is necessary to describe a stable liquid state (i.e. saturation). This is in agreement with the principle of minimum entropy production by Prigogine (1947) which generalizes the classical moderation theorem.

It is a well known fact of non-equilibrium thermodynamics, that thermal non-equilibria (e.g. heat supply) may evoke mechanical non-equilibria (e.g. pressure excess). Such phenomena are usually referred to as thermomechanical effects. From the previous analysis we postulate that a thermo-mechanical effect is present and some interesting consequences may serve as indirect proof of its occurrence.

3.2. Consequences for the macroscopic model

The model of separated flow has been modified to analyse the non-equilibrium process. In general this model consists of the three-dimensional sub-systems for vapour (g) and liquid (b). The saturation temperature of the vapour is $T_g = T_s(p_g)$ at the pressure $p_g = p_b$. The liquid temperature is $T_b \leqslant T_s(p_b)$. Our results suggest that we should now introduce an additional two-dimensional sub-system for the superheated‡ wall layer (w) in analogy to Ulrych (1976) but at a pressure which is simultaneously elevated to such an extent that its saturated temperature is $T_w = T_s(p_w)$. Mass and heat capacity are insignificant (figure 1). Each of these three sub-systems is supposed to be in thermodynamic equilibrium (lumped body model). Therefore the specific parameters, such as entropy s, enthalpy h, free enthalpy μ and volume $v = 1/\rho$ as well as the parameters of state T and p are properly defined. Non-equilibrium processes (i.e. heat flux $\dot{Q}'$ and mass flux $\dot{m}'$ per unit length) are only possible across the boundaries of the sub-systems:

---

†In section 6.1 it will be shown that the wall pressure p_w can reach up to 4.33 times the bulk pressure p_b (in the case of one-atomic coolants at DNB). On the one hand, this pressure difference is large compared to capillary pressure excess and justifies ignoring the latter, which until recently was the only contribution that had been considered. On the other hand, it is difficult to imagine how the pressure excess could reach these large values. Verification of this assumption can be given indirectly, when comparing the results of our whole theory with empirical information and thus it penetrates all of this study. Further emphasis of this hypothesis by various proofs has been given by Schroder-Richter (1991). It may be of particular interest to compare the measurements of the Leidenfrost temperature with predictions using the hypothesis of metastable superheating for the wall layer as originally proposed by Spiegler et al. (1963), and with a new prediction starting from the present hypothesis which has been performed by Schroder-Richter & Bartsch (1990). An extension to transition boiling has been performed by Huang et al. (1994).

‡Of course, this sub-system is not "superheated". Despite this fact, we will use some classical expressions in which we abbreviate the phrase "saturated at elevated pressure" in order to make the article easier to read.
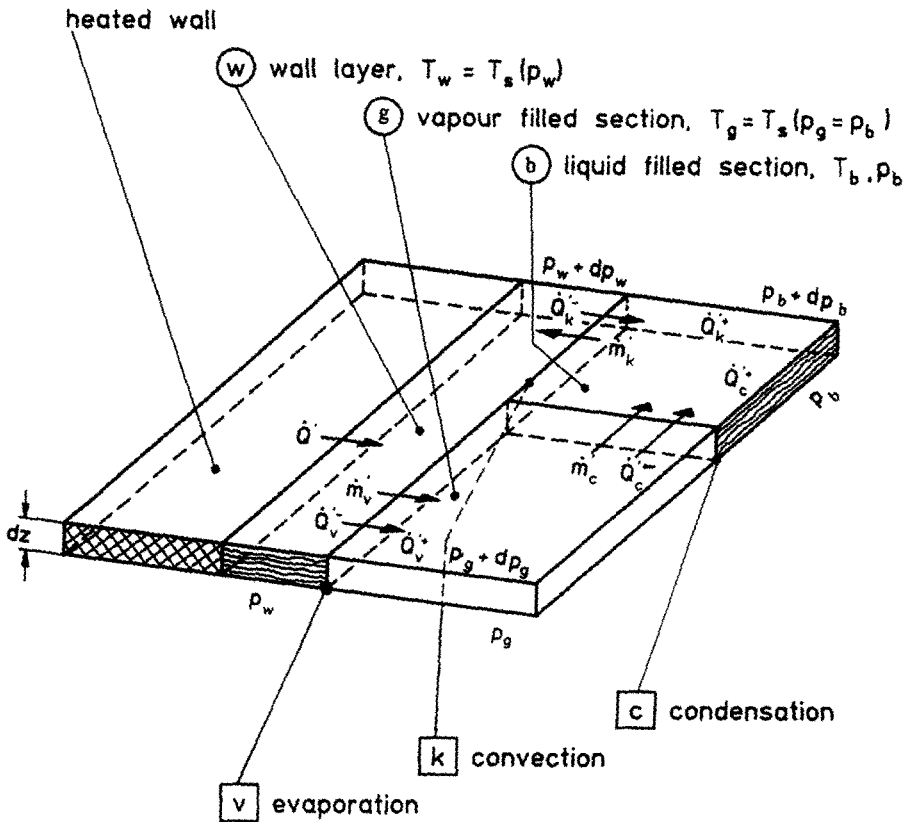
Figure 1. Macroscopic model of nucleate boiling.

evaporation (subscript v), convection (subscript k) and condensation (subscript c); input heat flux (superscript $+$), output heat flux (superscript $-$).

4. NON-EQUILIBRIUM THERMODYNAMICS AND THE CONSEQUENCES

The production of entropy [1] results from a balance of entropy. Linear non-equilibrium thermodynamics makes use of the equation by Gibbs and Duhem which has been adapted for open systems by de Groot & Mazur (1963):

$$T \frac{d(\dot{m}s)}{dz} = \frac{d(\dot{m}h)}{dz} - \mu \frac{d\dot{m}}{dz} - \frac{\dot{m}}{\rho} \frac{dp}{dz}, \qquad [10]$$

where $\dot{m}$ without the prime designates the total mass flow through the cross section of the flow channel. Using the first law of thermodynamics for the gradient of total enthalpy flow

$$\frac{d(\dot{m}h)}{dz} = \dot{Q}' + \left(\frac{\dot{m}}{\rho} \frac{dp}{dz} + \Psi' \right) \qquad [11]$$

and ignoring dissipation via friction Ψ' we find the gradient of total entropy for each sub-system

$$\dot{S}' = \frac{d}{dz}(\dot{m}s) = \frac{\dot{Q}'}{T} - \frac{\mu}{T}\dot{m}', \qquad [12]$$

where the heat fluxes $\dot{Q}'$ and mass fluxes $\dot{m}'$ result from the balances:

wall (w): $\qquad \dot{m}'_w = \dot{m}'_k - \dot{m}'_v, \quad \dot{Q}'_w = \dot{Q}' - \dot{Q}'^-_v - \dot{Q}'^-_k;$

vapour (g): $\qquad \dot{m}'_g = \dot{m}'_v - \dot{m}'_c, \quad \dot{Q}'_g = \dot{Q}'^+_v - \dot{Q}'^-_c;$

liquid (b): $\qquad \dot{m}'_b = \dot{m}'_c - \dot{m}'_k, \quad \dot{Q}'_b = \dot{Q}'^+_k + \dot{Q}'^+_c.$

4.1. Definition of the heat fluxes

Heat fluxes depend on further definitions related to the enthalpy constant if open systems are considered, cf. Muschik & Mueller (1983). The following relationships established input and output heat fluxes by definitions.

Reversible evaporation (v) is assumed in the superheated wall layer. Then the output heat flux is given by the first law for reversible processes, keeping in mind that the vapour produced has been assumed to be depressurized from p_w to p_g:

$$\dot{Q}_v'^- = \dot{m}_v' \left[\int_w^g dh - \int_w^g \frac{dp}{\rho_G} \right]. \tag{13}$$

where ρ_G designates the density of saturated vapour at any given pressure. Using the equation of Clausius–Clapeyron

$$\frac{dp}{dT} = \frac{h_{LG}}{T(v_G - v_L)}, \tag{14}$$

(where G and L designate the *saturated* vapour and liquid state) to substitute the integral of pressure by an integral of temperature, based on the definition $\dot{Q}_v' = \dot{Q}_v'^+ = \dot{m}_v' h_{LG}$ we get:

$$\dot{Q}_v'^- = \dot{m}_v' \left[h_{LG} + \int_g^w h_{LG} \frac{dT}{T} \right] = \dot{Q}_v' \left[1 + \ln\left(\frac{T_w}{T_g}\right) \right]. \tag{15}$$

Since the specific volume of liquid is small we ignore the mechanical work done to pressurize the liquid during recirculation to the wall layer after the bubbles have detached from the wall and we have:

$$\dot{Q}_k' = \dot{Q}_k'^+ = \dot{Q}_k'^-; \quad \dot{Q}_c' = \dot{Q}_c'^+ = \dot{Q}_c'^- = \dot{m}_c' h_{LG} \tag{16}$$

where condensation was assumed to proceed at constant pressure.

With the sum of entropy gradients in the sub-systems:

$$\dot{S}' = \dot{S}_w' + \dot{S}_g' + \dot{S}_b' = \Phi + \Omega \tag{17}$$

and [12] for each of the sub-systems the total gradient of entropy consists of an external supply

$$\Phi = \frac{\dot{Q}'}{T_w} \tag{18}$$

and an internal production

$$\Omega = \dot{Q}_v' \left[\frac{1}{T_g} - \frac{1}{T_w}\left(1 + \ln\left(\frac{T_w}{T_g}\right)\right) + \frac{1}{h_{LG}}\left(\frac{\mu_w}{T_w} - \frac{\mu_g}{T_g}\right) \right] + \dot{Q}_c' \left[\frac{1}{T_b} - \frac{1}{T_g} + \frac{1}{h_{LG}}\left(\frac{\mu_g}{T_g} - \frac{\mu_b}{T_b}\right) \right]$$
$$+ \dot{Q}_k' \left[\frac{1}{T_b} - \frac{1}{T_w} \right] - \dot{m}_k' \left[\frac{\mu_w}{T_w} - \frac{\mu_b}{T_b} \right]. \tag{19}$$

which must be positive according to the second law of thermodynamics. Now the source of entropy is written in a similar form to [1]. The fluxes J_i can be easily identified as heat fluxes and mass flux, whereas the driving forces may be rearranged to show their dependence explicit upon thermal non-equilibrium rather than specific free enthalpy.

4.2. Definition of the driving forces

The following considerations explain the enthalpy constant h_0 for the calculation $\Delta(\mu/T)$ with $(\mu - \mu_0) = (h - h_0) - T(s - s_0)$. In principle, the definition of h_0 is arbitrary, but it needs to agree with the definition of heat fluxes (Muschik & Mueller 1983) as $\dot{Q}_v'^+ = \dot{m}_v'(h_G - h_0) = \dot{m}_v'(h_{LG})$ and $\dot{Q}_c'^- = \dot{m}_c'(h_G - h_0)$. Ignoring conduction in the vapour phase (i.e. the vapour rests at saturation)

the definition $h_0 = h_L(T_g)$ fulfills this precondition (Schroeder-Richter 1991). We then have from the ideal gas approach using the isobaric heat capacity c_p:

$$\left(\frac{\mu_w}{T_w} - \frac{\mu_g}{T_g}\right) = \frac{h_L(T_w) - h_0}{T_w} - \frac{h_G(T_g) - h_0}{T_g} - (s_L(T_w) - s_G(T_g))$$

$$= \frac{-h_{LG}(T_w) + c_p(T_w - T_g) + h_{LG}(T_g)}{T_w} - \frac{h_{LG}(T_g)}{T_g}$$

$$- (s_L(T_w) - s_G(T_w)) - c_p \ln\left(\frac{T_w}{T_g}\right) + \frac{R}{M} \ln\left(\frac{p_w}{p_g}\right), \qquad [20]$$

which can be rearranged using the Clausius–Clapeyron equation [9] and $h_{LG} = T(s_G - s_L)$:

$$\left(\frac{\mu_w}{T_w} - \frac{\mu_g}{T_g}\right) = c_p\left[\frac{T_w - T_g}{T_w} - \ln\left(\frac{T_w}{T_g}\right)\right]. \qquad [21]$$

In a similar way using the heat capacity c_L for the liquid, we obtain:

$$\left(\frac{\mu_G}{T_g} - \frac{\mu_b}{T_b}\right) = c_L\left[\frac{T_g - T_b}{T_b} - \ln\left(\frac{T_g}{T_b}\right)\right]. \qquad [22]$$

Next [19] shall be rearranged to use [6] for the law of boiling heat transfer.

4.3. The phenomenological law of heat transfer

Now we use Taylor's series developed up to the second term

$$\ln\left(\frac{T_A}{T_B}\right) \sim \frac{T_A - T_B}{T_B} - \frac{1}{2}\left(\frac{T_A - T_B}{T_B}\right)^2 \qquad [23]$$

(letting A and B be arbitrary) to approximate the logarithmic expressions of [19], [21] and [22], which leads to the final representation of the entropy production during the irreversible process of flow boiling:

$$\Omega = \dot{Q}_v'\left[\frac{1}{2}\left(\frac{1}{T_w} + \frac{c_p}{h_{LG}}\right)\left(\frac{T_w - T_g}{T_g}\right)^2\right] + \dot{Q}_c'\left[\frac{1}{T_g}\left(\frac{T_g - T_b}{T_b}\right) + \frac{c_L}{2h_{LG}}\left(\frac{T_g - T_b}{T_b}\right)^2\right]$$

$$+ \dot{Q}_k'\left[\frac{1}{T_b} - \frac{1}{T_w}\right] - \dot{m}_k'\left[\frac{c_p}{2}\left(\frac{T_w - T_g}{T_g}\right)^2 + \frac{c_L}{2}\left(\frac{T_g - T_b}{T_b}\right)^2\right], \qquad [24]$$

where $\dot{Q}_v'$, $\dot{Q}_c'$, $\dot{Q}_k'$ and $(-\dot{m}_k')$ are addressed as fluxes J_i and the factors in brackets are the conjugated forces X_i according to [1]. A phenomenological law of heat transfer between the sub-systems can be obtained recalling the development to [6].

$$\dot{Q}_v' = L_{11}\left[\frac{1}{2}\left(\frac{1}{T_w} + \frac{c_p}{h_{LG}}\right)\left(\frac{T_w - T_g}{T_g}\right)^2\right] + L_{12}[\cdots] + L_{13}\left[\frac{1}{T_b} - \frac{1}{T_w}\right] + L_{14}[\cdots]$$

$$\dot{Q}_c' = L_{21}[\cdots] + L_{22}\left[\frac{1}{T_g}\left(\frac{T_g - T_b}{T_b}\right) + \frac{c_L}{2h_{LG}}\left(\frac{T_g - T_b}{T_b}\right)^2\right] + L_{23}[\cdots] + L_{24}[\cdots]$$

$$\dot{Q}_k' = L_{31}\left[\frac{1}{2}\left(\frac{1}{T_w} + \frac{c_p}{h_{LG}}\right)\left(\frac{T_w - T_g}{T_g}\right)^2\right] + L_{32}[\cdots] + L_{33}\left[\frac{1}{T_b} - \frac{1}{T_w}\right] + L_{34}[\cdots]$$

$$(-\dot{m}_k') = L_{41}[\cdots] + L_{42}[\cdots] + L_{43}[\cdots] + L_{44}\left[\frac{c_p}{2}\left(\frac{T_w - T_g}{T_g}\right)^2 + \frac{c_L}{2}\left(\frac{T_g - T_b}{T_b}\right)^2\right] \qquad [25]$$

Here we are interested in the wall heat flux alone

$$q = \frac{\dot{Q}_v' + \dot{Q}_k'}{P_h}, \qquad [26]$$

where P_h is the heated perimeter of the flow channel. Thus we arrive at the phenomenological law of total heat transfer:

$$q = B(T_w - T_g)^2 + K(T_w - T_b) + \frac{1}{P_h}[(L_{12} + L_{32})X_2 + (L_{14} + L_{34})X_4], \qquad [27]$$

where

$$B = \frac{(L_{11} + L_{31})}{2P_h T_G^2}\left(\frac{1}{T_w} + \frac{c_p}{h_{LG}}\right), \quad K = \frac{(L_{13} + L_{33})}{P_h T_w\, T_b},$$

are new coefficients independent of fluxes and forces.

This law should be valid for boiling with forced convection between both onset of and departure from nucleate boiling, as far as our assumptions hold. Particular attention should be paid to the assumption of a saturated wall layer at elevated pressure (i.e. as far as the void fraction remains low). Passing through the analysis [13] and [15] or [20] and [21] and keeping in mind [23] to convert [19] into [24] and [25] we see that the non-linear coupling of heat flux q with wall superheat $(T_w - T_g)$ results from the mechanical non-equilibrium alone. The driving force of boiling is $X_1 = BP_h/(L_{11} + L_{31})(T_w - T_g)^2$. It can be easily seen from a similar analysis that the classical assumption of constant pressure leads to linear coupling between q and ΔT according to Newton's law of cooling at constant heat transfer coefficient which is known to hold at single-phase flow alone. We recall the development to [6] as a demonstration that the phenomenological coefficients L_{ik} may neither depend on q nor on $(T_w - T_g)$.

4.4. Comparison of the boiling analysis with empirical knowledge

Thermodynamics of irreversible processes is usually applied with the final fitting of the phenomenological coefficients to empirical information. This could lead to new correlations of boiling heat transfer, but this comprehensive work deals with data inspections far away from the purpose of this study. For the interested reader it should be mentioned that the influence of mass flow on boiling heat transfer is related to the dissipation by friction Ψ' in [11], which had to be restored to the balance of entropy if an adequate phenomenological law is analysed. In fact, flow boiling is a complex phenomenon and can be governed by several parameters apart from those selected here.

As mentioned above, we will concentrate on the effect of mechanical non-equilibrium on the power of the wall superheat. This describes the boiling heat transfer at forced convection if the void fraction remains low. In this case, in particular, the correlation by Thom et al. (1965) is recommended by Groeneveld & Snoek (1986) for water and by Celata et al. (1986) for refrigerant R12. This correlation readily compares with the phenomenological law [27], if

$$\left(\frac{T_w - T_g}{T}\right)^2 \gg \frac{T_w - T_b}{T}$$

and Thom et al. (1965) have obtained:

$$B = 1970\,\frac{W}{m^2 K^2}\exp\left(\frac{P_b}{4.34\,\text{MPa}}\right).$$

The second power of the wall superheating has been determined empirically and agrees with the analytical result [27], but it has not been generally accepted. Most of the flow boiling correlations indicate higher exponents (which conflict with the hypothesis of constant pressure as well, since we obtained Newton's law in that case); e.g. Tong & Weisman (1979) mentioned that Thom et al. (1965) used a database with low heat fluxes whereas the higher exponent could be valid close to the critical heat flux. This is credible, since these high heat fluxes usually suggest that a high void fraction could be produced as long as other flow parameters such as high sub-cooling, high flow rate short flow channel etc., do not compensate for this effect. In the case of high void fraction the flow regime is annular and thus outside our model assumptions.

In most of the practical cases the true void fraction is unknown and thus not listed with the numerous correlations and data of the literature. The data mentioned above by Thom et al. (1965)

have been obtained and combined with measurements of void fraction using a gamma densi-tometer. Their results indicate low void fraction for most of the data.

Next we consider the correlation by Chen (1963):

$$q = SB_c(p_w - p_g)^{0.75}(T_w - T_g)^{1.24} + FK_c(T_w - T_b),$$

$$B_c = 0.00122 \frac{k_L^{0.79} c_L^{0.45} \rho_L^{0.49} g^{0.25}}{\sigma^{0.5} \eta_L^{0.29} h_{LG}^{0.24} \rho_G^{0.24}},$$

$$K_c = 0.023 \frac{k_L}{d_h} \text{Re}^{0.8} \text{Pr}^{0.4}, \qquad\qquad [28]$$

where k_L, g, σ, η_L, d_h, Re and Pr designate heat conductivity of liquid, acceleration due to gravity, surface tension, dynamic viscosity of liquid, hydraulic diameter, Reynolds number and Prandtl number, respectively. The boiling suppression factor S and the Reynolds number factor F can be read from diagrams by Chen (1963). This correlation holds for flow boiling of water, methanol, cyclohexane pentane, heptane and benzene, but was suggested at saturation ($T_g = T_b$) alone. Thus we have rearranged the original superposition of heat transfer coefficients by Chen (1963)

$$\frac{q}{T_w - T_b} = \frac{\dot{Q}'_v/P_h}{T_w - T_g} + \frac{\dot{Q}'_k/P_h}{T_w - T_b}$$

into a superposition of heat fluxes [28] which compares with the formalism of [27].

Note that a simple superposition of heat transfer coefficients during pool boiling and single-phase convection makes use of the unjustified assumption of disappearing cross coefficients L_{13} and L_{31} in [25] and [27]. Instead of adding the overlapping effects Chen (1963) introduced the correction factors.

An interesting fact may be that Chen (1963) uses the difference of saturation pressures corresponding to T_w and T_g to correlate the boiling heat transfer even if it is explained in a somewhat different way. If we linearize [14]

$$\frac{p_w - p_g}{T_w - T_g} \sim \frac{h_{LG}}{T(v_G - v_L)}$$

to substitute the pressures of [28] by temperatures, we readily rediscover our analytical result [27] with

$$B = SB_c \left(\frac{h_{LG}}{T(v_G - v_L)} \right)^{0.75}, \quad K = FK_c \qquad\qquad [29]$$

At low void fraction the thermodynamic equilibrium quality is very small and we read from the diagrams by Chen (1963) that F approaches one and thus S is a constant depending on the Reynolds number, i.e. F and S are independent of heat flux and temperature differences as requested for the phenomenological coefficients L_{ik} of [6].

Further comparisons of [27] with empirical information have been performed by Schroeder-Richter (1991). These showed that the exponent of the wall superheat approaches two if the underlying data or correlations clearly indicate low void fraction and the exponent tends to be higher if the true void fraction is high or unknown. It should be mentioned that an honorable data analysis by Cooper (1989) did not result in sufficient measurements of nucleate flow boiling to clearly indicate whether two or three is the correct exponent, but he preferred three. Bartsch et al. (1990) made a first attempt to explain the exponent three for pool boiling based on the present analysis.

The thermodynamics of irreversible processes does not necessarily determine that the coefficient B is of finite value. It is possible that Taylor's series [3] starts with second or third order terms. Thus higher exponents than two for the wall superheat are not strictly excluded by our theory. The analysis mainly shows that *the exponent is not one!* Of course, the remaining statement is not new, but the present analysis seems to be the first attempt to explain the non-linear law of heat transfer using analytical tools alone. This in turn, emphasizes the postulated mechanical non-equilibrium and is referred to in our comments following [27].

Here we interrupt the discussion and postulate again that the mechanical non-equilibrium $(p_w - p_g)$ as described above will prevail up to DNB. It seems to be of particular interest to apply the balance of momentum to the interfaces of a single bubble and to analyse which consequences will be indicated, if the pressure difference is large.

5. BALANCE OF MOMENTUM AND DNB CONDITIONS

Photographs of the boiling process taken with a high speed camera show, for a growing vapour bubble at heat fluxes close to DNB, that

(1) initially the bubbles are not shaped hemispherically as observed at lower heat fluxes, but are shaped like a coin with flat interfaces both at the bottom close to the heated wall and at the top;

(2) between the heated wall and the bottom of the bubble there is a thin liquid microlayer which rests at the heated wall without visible deformation;

(3) the top of the bubble spreads in a shape like an umbrella and grows into the flow rapidly;

(4) when the bubble reaches the shape of a hemisphere the base is laced and the bubble detaches from the heated wall like a mushroom.

5.1. Microscopic model and balance of momentum

The first observation suggests a new model of one-dimensional parallel flow (normal to the heated wall) at constant velocity w_r (lumped body model). Assuming that within the microlayer (w) between the heated surface and the vapour (g) of each bubble there is a motionless liquid ($w_w = 0$), the steam produced moves away from the microlayer within the velocity w_g in accordance with figure 2. The interface (I) moves at the velocity $w_I < 0$ towards the heated surface. Therefore the steam can be considered to move at a velocity $w_{gI} = w_g - w_I$, if measured relative to the interface I.

The interface (II) at the top of the bubble is directed towards the centre of the fluid. Thereby the covering liquid (t) is pushed away at a lower speed $w_t < w_{II}$ if evaporation can be assumed in the interface (II). This motion is a secondary flow and considered to be a free-jet with respect to the liquid bulk flowing axially through the channel, since it is distinctly governed by thermally-induced evaporation rather than an arbitrary turbulent vortex. The static pressures are Π_w, Π_g and Π_t in the microlayer, the steam and the turbulent jet on top of the bubble, whereas the pressures
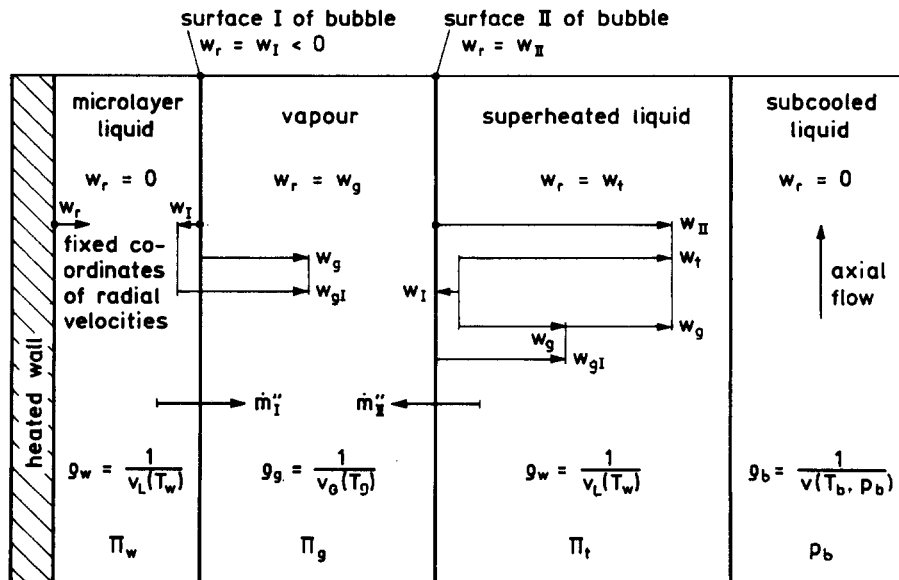

Figure 2. Microscopic model of an initially flat bubble at high heat fluxes. Velocities of sub-systems and interfaces.

in the sense of thermodynamic properties of state are designated by p_w, p_g and p_t, respectively. Prigogine (1947) has shown that it is necessary to distinguish these definitions of pressure, if sub-systems are moved at different velocities and we will see what this means when advancing through this chapter.

Using these definitions we can write balance equations which are valid at the interfaces. Noting that no gradients exist via the singular surfaces, these balance equations are usually obtained as jump conditions which are based on the hypothesis that conserved properties as mass, momentum etc. will disappear from one side of the surface at the same rate as they leave at the opposite side, as long as the surface does not store this property, e.g. Mueller (1985). For the mass fluxes $\dot{m}''$ passing the interfaces we obtain:

$$\dot{m}_I'' = \rho_w(w_w - w_I) = \rho_g(w_g - w_I), \tag{30}$$

$$-\dot{m}_{II}'' = \rho_g(w_g - w_{II}) = \rho_w(w_t - w_{II}), \tag{31}$$

where the thermodynamic states of both the liquid microlayer (w) and the liquid free-jet (t) are taken to be identical since we consider the situation according to our first observation immediately, i.e. when both the liquid systems have lost thermal contact. At this moment the driving forces across both of the interfaces are still equal and it seems reasonable to assume equal fluxes as well:

$$\dot{m}_I'' = \dot{m}_{II}''. \tag{32}$$

More attention must be paid to the balances of momentum, if the interfaces are compared either thermodynamically or mechanically. Since momentum is a vector its component normal to the interface results from multiplying the unit normal n_I and n_{II}, respectively. From the thermodynamical point of view all the input to a sub-system (e.g. vapour) is positive and we have:

$$p_w + \rho_w w_w(w_w - w_I) = p_g + \rho_g w_g(w_g - w_I), \tag{33}$$

$$p_t + \rho_w w_t(w_t - w_{II}) = p_g + \rho_g w_g(w_g - w_{II}). \tag{34}$$

On the other hand, a superposition of balances is possible only if the balances are taken for the same system of coordinates, i.e. n_I and n_{II} do not lie in opposite directions but in identical directions. From a mechanical viewpoint we have:

$$\Pi_w + \dot{m}_I'' w_w = \Pi_g + \dot{m}_I'' w_g, \tag{35}$$

$$\Pi_t + \dot{m}_{II}'' w_t = \Pi_g + \dot{m}_{II}'' w_g, \tag{36}$$

where capillary forces (resulting from surface tension) are not disregarded. This physically does not occur since we observed flat interfaces (cf. observation 1).

In this case we are interested in the total pressure difference between the unknown pressure at the wall and the given system pressure in the bulk of the liquid p_b. Thus we start from [35] and [36] and the superposition reads

$$\frac{w_t^2}{2} = 2w_g^2 = \left(\frac{1}{\rho_g} - \frac{1}{\rho_w}\right)(\Pi_w - \Pi_t), \tag{37}$$

where the velocities are substituted using [30], [31] and [32], cf. vector diagram in figure 2.

We now replace the static pressures with thermodynamic properties of state, which do not have to depend upon the velocity at which an arbitrary observer is moved or not (criterion of objectivity). Prigogine (1947) demonstrated that the thermodynamic pressure agrees with the static pressure, if the latter is measured by an observer who is moved at the baricentric velocity of the sub-system. This condition holds for the microlayer which is unmoved with respect to fixed coordinates at the heated wall that underly the present analysis. In contrast, the static pressure Π_t of a free-jet is usually assumed to be in mechanical equilibrium with the environment p_b, which is known as Torricellis' boundary condition of a free jet, cf. figure 3.
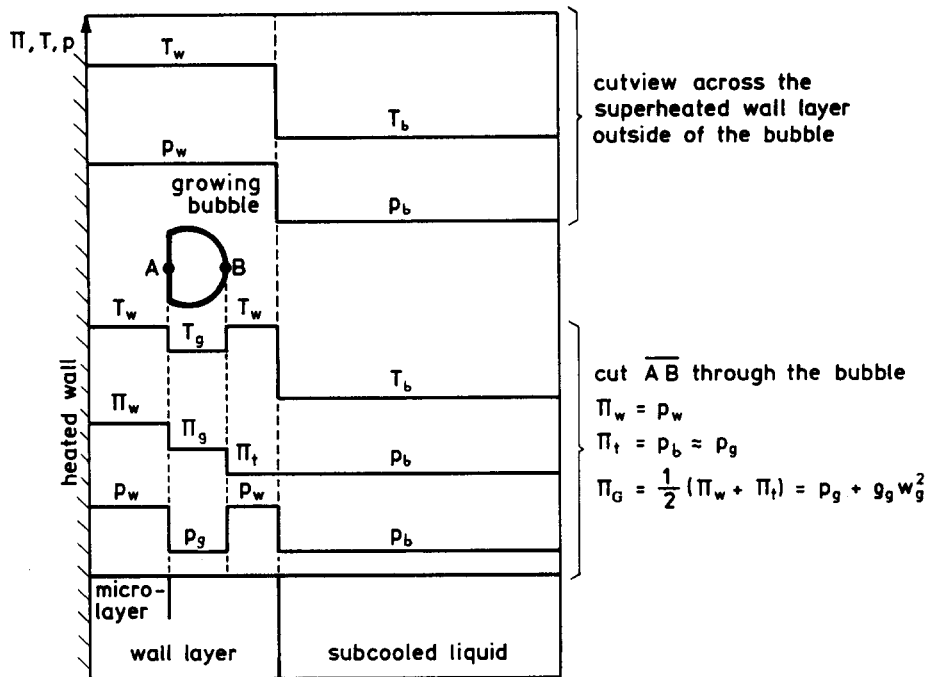
Figure 3. Microscopic model. Radial distribution of temperature and pressure.

Imagine another observer moving with the liquid on top of the bubble who is baricentric with respect to the system (t) and can thus measure the static pressure of (t) equal to p_w, while the wall layer seems to have a lower pressure p_b, cf. Prigogine (1947). However, the static pressures Π of [37] can be substituted by thermodynamic pressures

$$\frac{w_t^2}{2} = 2w_g^2 = (v_g(T_g) - v_L(T_w))(p_w - p_b) \tag{38}$$

since we used fixed coordinates at the wall and keeping in mind that we have assumed saturated states for both wetting liquid at the heated wall (w) and vapour (g), the reciprocal densities are replaced by saturated specific volumes at different temperatures.

5.2. Consequences at DNB conditions

Looking for a maximum condition for either of the velocities w_g or w_b, respectively, we are reminded of a convergent–divergent nozzle. The maximum mass flux through the nozzle is reached if the velocity in the smallest cross section equals the speed of sound.

Applying this limit to the present model of parallel flow we identify any cross section of equal value and the differences between the velocities w_w, w_g, w_t are the only velocities of the material which fulfil the criterion of objectivity. Thus we find that the difference between w_w and w_t is maximum and the sum of the mass fluxes $(\dot{m}_I'' + \dot{m}_{II}'')$ is limited, if it equals the speed of sound of a saturated liquid a_L:

$$w_t - w_w = w_t = a_L(T_w). \tag{39}$$

On the other hand, the speed of sound of a saturated vapour a_G is found to be lower and it might occur that both the equal differences

$$w_g - w_w = w_t - w_g = w_g = a_G(T_g) \tag{40}$$

define both the maxima of the mass fluxes $\dot{m}_I''$ and $\dot{m}_{II}''$ at the same time but before condition [39] can be reached. In fact, the evaporating mass flux will be limited by the first of the conditions [39] and [40] that can be reached with increasing velocities $w_t = 2w_g$.

The following assumptions suggest that several different maxima occur simultaneously with the limiting mass flux which could cause a special type of critical heat flux:

(1) The surrounding liquid temperature is strongly related to the time average of the wall temperature at the initial bubble formation (first observation) after an infinite waiting time between detachment of the last bubble and formation of the considered one. The later bubble growth is as fast as the necessary enthalpy of evaporation is supplied which is mainly contributed from stored energy rather than from the heated surface during the rapid process. Since the stored energy is determined by the liquid temperature (and pressure) at the initial state, the bubble growth is predetermined by the average wall temperature for most of its growth period, although the later growth of the bubble proceeds slower and at lower values of T_w and p_w.

(2) Above we have assumed the maximum mass flux to a single bubble during its period of growth. The bubble is taken to be a suitable average to represent the maximum mass flux to the whole bubble ensemble $\dot{m}'_v$ simultaneously, though its value is much lower since the bubbles do not cover the whole heat transfer surface.

(3) A maximum heat flux of evaporation $\dot{Q}'_v = h_{LG}\dot{m}'_v$ is given at the same time.

(4) Convection heat flux $\dot{Q}'_k$ is significantly enhanced, if bubbles grow fast since this serves for intense mixing between the superheated wall layer and the sub-cooled liquid bulk. Then a maximum of convection heat flux is simultaneously given and by definition [26] the total heat flux reaches a maximum as well.

A maximum boiling heat flux is usually called critical heat flux. We strongly restrict this result to *DNB instead of dry-out* since the analysis is based on bubble models which are only suitable at very low true void fraction!

Now we rearrange the balance of momentum [38] at either of the DNB conditions [40] or [39]:

$$[v_G(T_g) - v_L(T_w)][p_s(T_w) - p_s(T_g)] = 2a_G^2(T_g), \qquad [41]$$

if $2a_G(T_g) \lessgtr a_L(T_w)$,

$$[v_G(T_g) - v_L(T_w)][p_s(T_w) - p_s(T_g)] = \tfrac{1}{2}a_L^2(T_w), \qquad [42]$$

if $2a_G(T_g) \gtrless a_L(T_w)$,

noting that the pressures have been assumed to be saturation pressures at different temperatures T_w and T_g according to the model. Obviously, both of the results compare properties of saturated states which all depend on the two temperatures T_w and T_g alone. Hence, the wall temperature T_w can be calculated iteratively from [41] and [42] using a suitable table of state, bearing in mind that the saturation temperature $T_g = T_s(p_g)$ is usually given by the system pressure p_b and $p_g = p_b$. Starting from thermal equilibrium the lower temperature [41] or [42] is the first sonic limit that will be reached and thus predicts the wall temperature at DNB. We will see that [41] is a low pressure condition whereas [42] is valid at higher pressures.

At low pressure it may be convenient to apply an ideal gas approach

$$a_G(T_g) = \sqrt{\kappa_G(T_g)p_s(T_g)v_G(T_g)}, \quad v_G(T_g) = \frac{R}{M}\frac{T_g}{p_s(T_g)} \gg v_L(T_w)$$

to the DNB condition [41] if properties of state are not given completely or an explicit calculation is necessary and we result either in the wall pressure at DNB

$$p_w = p_{DNB} = (2\kappa_G + 1)p_b \qquad [43]$$

or using the Clausius–Clapeyron equation [9] we have

$$T_{DNB} = \left[1 - C\frac{T_g}{h_{LG}}\right]^{-1} T_g, \quad C = \frac{R}{M}\ln(2\kappa_G + 1), \qquad [44]$$

where

$$\kappa_G = -\frac{v}{p}\left(\frac{\partial p}{\partial v}\right)_s \sim \begin{cases} 1 + 2/3 \text{ one-atomic coolants} \\ 1 + 2/5 \text{ two-atomic coolants} \\ 1 + 1/3 \text{ three-atomic coolants} \\ 1 + \cdots \text{ multiatomic coolants.} \end{cases} \qquad [45]$$

Neither an idealized nor an explicit calculation is available at elevated pressure, but it is very easy to solve T_{DNB} from [41] and [42] by trial and error. In this way our model will be verified using documented measurements of wall temperatures at DNB.

6. COMPARISON OF THE DNB ANALYSIS WITH DOCUMENTED MEASUREMENTS

We have developed an analytical model that predicts wall temperatures at DNB from properties of state without using empirical coefficients. Physical models of such type should hold for any boiling fluid. Thus, a suitable verification becomes more significant with the number of fluids rather than with the number of measurements for a single fluid that are considered. Thus we start our verification considering a variety of fluids of different chemical nature, for simplicity and with respect to available data at moderate pressure. We then extend this analysis to the pressure effect by picking out some refrigerants, water and potassium where documented measurements as well as properties of state are available and complete enough to be handled in this way.

6.1. Effect of molecular constitution

The sonic limits [39] and [40] represent very fast boiling velocities which are certainly somewhat difficult to accept. The physical nature of this assumption focuses particular attention on the number of atoms which constitute a molecule of the boiling fluid, since this seems to remain as the sole parameter reflecting the chemical nature of the boiling liquid which could affect the DNB limit ([43] and [44]) under idealized low pressure conditions. Thus we start our verification by a chemical survey (table 1) and consider one fluid as an example for each number of atoms which allows for an idealized calculation of the isentropic exponent κ_G.

Deviating from our model predicting DNB in the case of sub-cooled flow boiling, we found pool boiling measurements for most of the documented literature except water. On the other hand, this is no disadvantage, since table 1 exhibits a very small deviation between our predictions and these

Table 1. Wall temperatures corresponding to DNB affected by the speed of sound at different molecular constitutions. Documented measurements compared with analytical prediction

Fluid and boiling mode	Atoms per molecule	$2\kappa_G + 1$	M (kg/kmol)	C (kJ/kg K)	Measured p_b (MPa)	Measured T_{DNB} (K)	Calculated T_{DNB} (K)	Authors of measurement, properties of state
Argon, pool boiling	1	4.33	40	0.31	0.108	106 108 109	106¶	Kosky & Lyon (1968) Rabinovich et al. (1987)
Nitrogen, pool boiling	2	3.8	28	0.4	0.1 0.1	91§ 91	91¶	Merte & Clark (1964) Sychev et al. (1987a)
Water, flow boiling	3	3.67	18	0.6	0.11	416	417¶	Johannsen & Weber (1988) Schmidt (1982)
Benzene, pool boiling	12	3.2‡	78.1‡	0.125	0.013 0.240	335 441	329¶ 442¶	Kutateladze et al. (1973) Vargaftik (1975)
Caesium, pool boiling	1–2†	function of pressure†			0.004	983–993	989‖	Kutateladze et al. (1973) Vargaftik (1975)

†A chemical reaction, 2Cs ⇆ Cs$_2$ associates with the boiling process.
‡Data by Schaafs (1967).
§Both, standard and near zero gravity.
¶Calculated from [44].
‖Calculated from [41].

measurements. In turn, the favourable result motivates to extend our theory to pool boiling conditions as far as the critical boiling condition is considered. Obviously, evaporation in a pool proceeds bubbly but shows no similarity to the dry-out phenomenon. Thus all the modelled sub-systems of figure 2 are present to calculate pool boiling in a similar way.

Inspecting table 1 with respect to our new hypothesis for the thermodynamic state of the liquid microlayer we read a maximum of 4.33 times the bulk pressure for argon. This considerable non-equilibrium between the pressures at the horizontal heat transfer surface and the fluid level might mislead us to the conclusion that, if the theory is true, then the whole fluid content should be vertically ejected from the experimental facilities. Such a take off by the fluid has never been observed under these circumstances [though we know from Leidenfrost (1756) about sputtering of liquid drops when brought into contact with a hot plate]. However, the wrong expection adopts a strictly static and lumped point of view to the integral balance of momentum at the pool which is much too simple. In fact pool boiling is a highly dynamic and multi-dimensional process with bubbles rising and liquid flowing in reverse which could be considered as a harmonic game between waves of temperature and swinging fluid motion. Locally high wall temperatures initiate bubble formation and then rising vapour as modelled. Thereby the wall temperature is cooled which is connected with a lower pressure of saturation in the wall layer. Thus the surrounding liquid falls back under gravity and then re-wets the solid. In this sense our theory is not in conflict with observations of pool boiling. For argon, as mentioned above, three measurements by Kosky & Lyon (1968) scatter above our prediction.

It should be mentioned that we have not yet compared our theory with argon measurements at elevated pressure, since no speed of sound data were available except our ideal gas approach. More impressive is the fact that DNB temperatures for nitrogen have been reported by Merte & Clark (1964) at standard and near-zero gravity and both identical measurements compare with the prediction up to the decimal point. This precisely reproduced measurement clearly indicates that the possible influence of gravity on critical surface temperatures could be sub-ordinate or does not occur. This might indicate a justification that our balances of momentum ([35] and [36]) are well formulated and we are afraid that usual models of bubble dynamics could count negligible parameters only when balancing capillary forces against hydrostatic pressure gradients as far as the very initial state of bubble formation is concerned. Surely the order of magnitude between these pressure effects will reverse if a later stage of the bubble growth period is to be considered. Particularly at bubble detachment ($\dot{m}_I'' = \dot{m}_{II}'' = 0$) we obtain zero balances using [35] and [36] and the remaining forces are capillary and hydrostatic, which is consistent with the honorable work by Mitrovic (1983).

However, a single measurement should not emphasize extended discussions on gravity. Other nitrogen measurements, have been reported at less precision, e.g. Kosky & Lyon (1968) reported that it has been impossible to reproduce their own measurements. Thus we did not try to include them in table 1.

Worse measurements of benzene and caesium are predicted which may be addressed by both a lower precision of measurement as avowed by Kutateladze et al. (1973) and difficult estimation of the properties of state, cf. section 6.3. A single water measurement has been picked out arbitrarily, but this fluid deserved discussion in a separate section.

6.2. Pressure effect on DNB temperatures of water

Water is the most frequently used cooling liquid and thus comprehensive data banks exist showing several flow parameters of technical relevance which describe the CHF conditions. Thus we must report on the incredible fact, that these technical parameters can be cumbersomely converted to the necessary physical parameters describing our model for only very few of these data. Note that our model predicts wall temperatures at DNB, whereas CHF measurements are frequently reported without these temperatures. Due to imperfect thermal contact of thermocouples with the flow channel and inhomogeneity of the tube material when thermocouples are embedded etc., it is difficult to calibrate wall temperatures. Thus thermocouples have been frequently used to indicate the abrupt temperature rise when CHF is over-ridden leaving all information concerning exact wall temperatures out of consideration.

Thus only calibrated and reported wall temperature measurements can be used for comparison. Unfortunately, most of the remaining CHF measurements cannot be compared with our model since it only predicts the DNB type rather than the dry-out type of critical boiling mechanisms. (The wall temperature corresponding to dry out tends to be much lower than our prediction and depends on flow parameters as well as axial position in the heated channel or rod respectively.) Moreover, the physical parameter governing the separation of phases from bubbly to annular flow is the true void fraction. With very few exceptions, the true void fraction remains unknown throughout the experiments since it depends on such measurable quantities as inlet sub-cooling and the supplied wall heat flux in a complex and not yet successfully understood manner. Among others there is the problem of the unknown slip ratio between the axial velocities of both vapour and liquid phases and there is also the problem that an unknown fraction of the supplied heat contributes to an increase in the enthalpy of the sub-cooled liquid whereas the remaining part contributes to an increase in the void fraction which is to be estimated. On the other hand, saturated inlet conditions to the flow channel will lead to annular flow via a short path through the channel since the high CHF serves for intensive vapour production. Thus we have to use the sub-cooled boiling data even though we cannot predict the corresponding true void fraction exactly. Finally, there is no distinct quantity of void fraction below which the DNB mechanism can be separated from the dry-out mechanism above. In spite of this, the two mechanisms are continuously overlapping each other whereas we have modelled the proper nature of DNB which should find its applicability as long as we consider the limiting case of disappearing void fraction.

All of these arguments above illustrate that a proper selection of documented data is necessary to make the following verification significant. On the other hand, any selection of data has to be justified clearly, if the comparison with our model is to be of value. Since any single measurement has to meet all the conditions above, it cannot be sufficiently reported here. The interested reader will find the necessary details in Schroeder-Richter (1991).

In this paper we jump to the readily selected data and compare them with our model. In this way, figure 4 shows the two temperatures of saturation for both the superheated wall layer versus vapour according to our model. Temperatures between the triple point and critical point are scaled on either side of the diagram using celsius or kelvin which then covers any combination of the two saturated states that could occur.

Calculations using [41] and [42] are shown in figure 4. We used the properties of water from Schmidt (1982) and completed with the speed of sound data by Elsner et al. (1982). The lower temperature of both calculations is the first limit reached when heating up the wall from thermal equilibrium ($T_w = T_g$) and thus represents the final prediction of DNB (heavy solid line). This gives a result where the speed of sound of vapour constitutes the true limit below about $T_g = 200°C$ (corresponding to low or moderate pressure) whereas nucleate boiling is terminated by the liquid exceeding its speed of sound if the vapour temperature (respectively pressure) is higher.

At higher wall temperatures stable or unstable film boiling is expected. We obtain nucleate boiling between the heavy line and the diagonal as long as the onset of nucleate boiling has occurred, whereas the region below corresponds to single-phase convection.

In a practical sense we usually know the system pressure rather than the vapour temperature. Therefore the corresponding pressure is scaled on the diagonal with a vertical connection to the vapour temperature and horizontal connection to the wall temperature. An example is drawn showing how to get from the system pressure (about 20 kPa) to the condition of DNB and then how to reach the elevated pressure in the liquid wall layer. This is about 80 kPa which represents considerable mechanical non-equilibrium. Nevertheless, the selected data are well predicted by our model over the range from close to triple pressure up to about 7 MPa.

It should be mentioned that we used the flow boiling measurements of Johannsen & Weber (1988), with additional unpublished information by the authors, which enabled adequate data selection. Further measurements by Howard (1976), Shires et al. (1964), Bennett et al. (1966) and Eliott & Rose (1970) have been obtained by quenching a dry vertical rod. These authors published diagrams on the velocity of the quench front versus the temperature of the rod surface showing a distinct trend to infinite velocity at a particular wall temperature. We obtain the results that the infinite velocity of the quench front seems to have a real sense only if the rod is not wetted axially
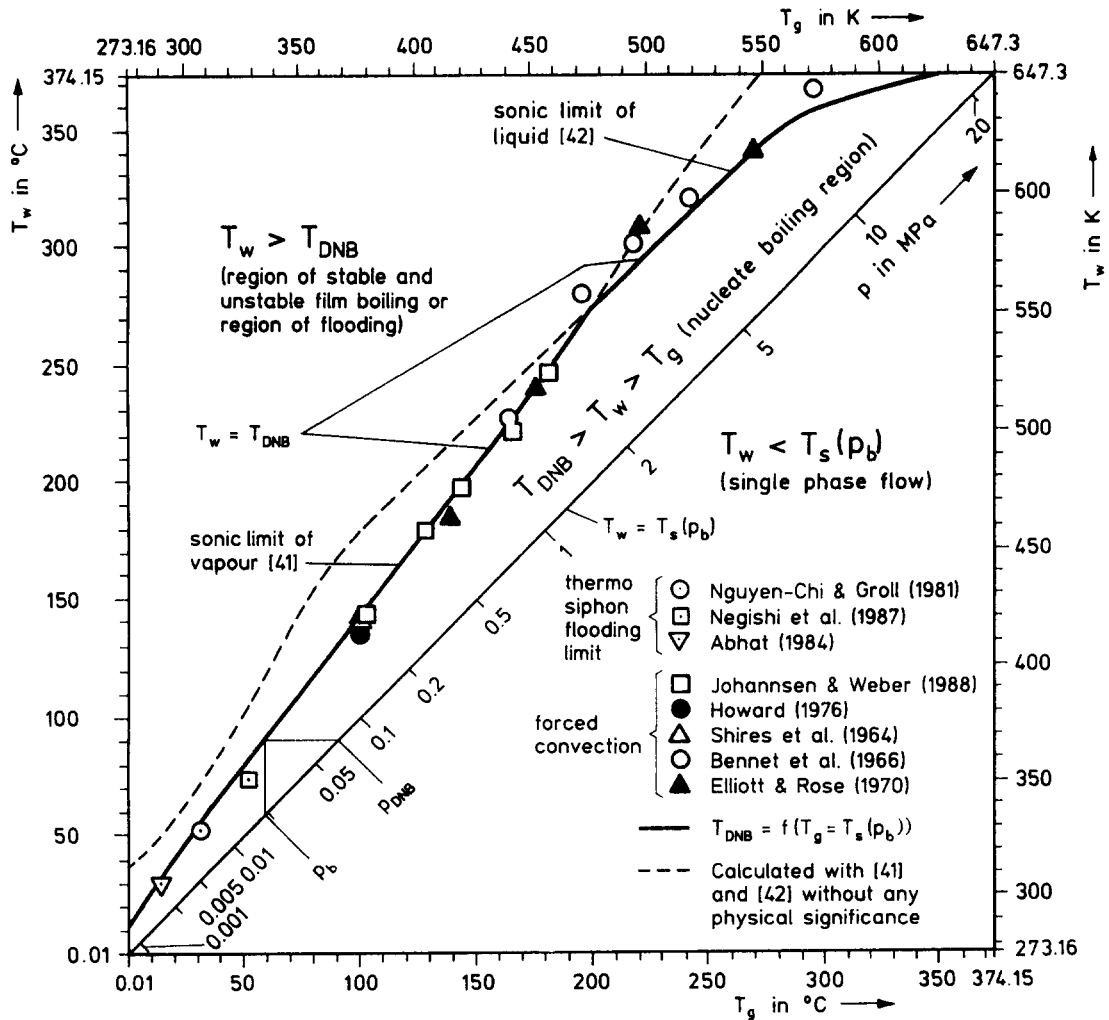
Figure 4. Effect of radial pressure differences on T_{DNB} versus saturation temperatures $T_s(p_b) = T_g$ for flow boiling, quenching and thermosiphon flooding with water.

but radially for all axial levels at the same time. This, of course, can only take place if the bulk flow is filled with the liquid phase which is a low void fraction condition and thus corresponds well with our theory. A further group, the sub-atmospheric measurements, has been reported for copper water thermosyphons, partly from flooding phenomena. Individual argumentation has been collected to estimate a DNB limit and has concluded that the measurements could not be converted into DNB temperatures without losing accuracy, e.g. delay of the thermocouple reading with respect to heat capacity. We are therefore surprised that the pressure extrapolation is well described down to the triple point. Finally we should not worry about the few water measurements that have been used from intensive literature studies. More valuable proof of our theory could be given by analysing other fluids in similar way.

6.3. Pool boiling of refrigerants and liquid metals

There is no doubt that peak heat fluxes during pool boiling correspond to DNB in general. Consequently there is no need to select these measurements from dry-out phenomena and we use data sets as a whole for the following. Section 6.1 readily ruled out that [41] and possibly [42] could hold for different geometries of the boiling process (i.e. pool boiling in addition to primarily forced convection modelling) and for different liquids, since [41] and [42] are deduced analytically using balances of mass and momentum, that are neither restricted to a particular geometry nor to a particular liquid.

Kosky & Lyon (1968) investigated pool boiling of different condensed gases. Heat flux versus super-heating diagrams are shown including the condition of critical boiling, called "peak nucleate boiling flux". We estimated the corresponding peak nucleate boiling temperatures by graphical measurement using these diagrams. The data set covered the fluids nitrogen, oxygen, argon, methane, carbon tetrafluoride (CF_4 or R14), helium and some mixtures. So far, we have no theory for mixtures and therefore leave these data out of consideration. Problems with the use of nitrogen and argon data have been discussed in section 6.1, but the remaining data set has been used completely by Schroeder-Richter (1991).

First, the oxygen data have been inspected and plotted in figure 5, which is a similar diagram to figure 4 showing the triple point in the lower left corner and the critical point in the upper right-hand side. Thermodynamic properties (including speed of sound data) have been taken from Sychev et al. (1987b). The measurement data are well predicted in both the ranges where [41] or [42] is applicable.

Next we used the data set of methane. Unfortunately, not all of these data could be reproduced. Thus the authors did not publish five of their measurements, cf. Kosky & Lyon (1968).

We have listed all of the acceptable, and therefore published, data in table 2 using propeties of state from Sychev et al. (1987c) for analytical prediction. The first three lines show experimental data scattering around our analytical result where the speed of sound of vapour defines the DNB limit. At 1.641 MPa our model indicates that we need the speed of sound of liquid methane in the narrow region of the thermodynamic critical state. It is characterized by strongly reduced liquid speeds of sound with slight elevation of the corresponding temperature of saturation. Sychev et al. (1987c) reported that our knowledge about speed of sound data still exhibits large uncertainties in this range but we concluded that our prediction of wall temperatures using [42] is extremely sensitive to uncertainties in speed of sound data. Therefore, we are not disappointed with our theory which deviates by 7.7 K from a measurement which is reported with considerable uncertainty as well.
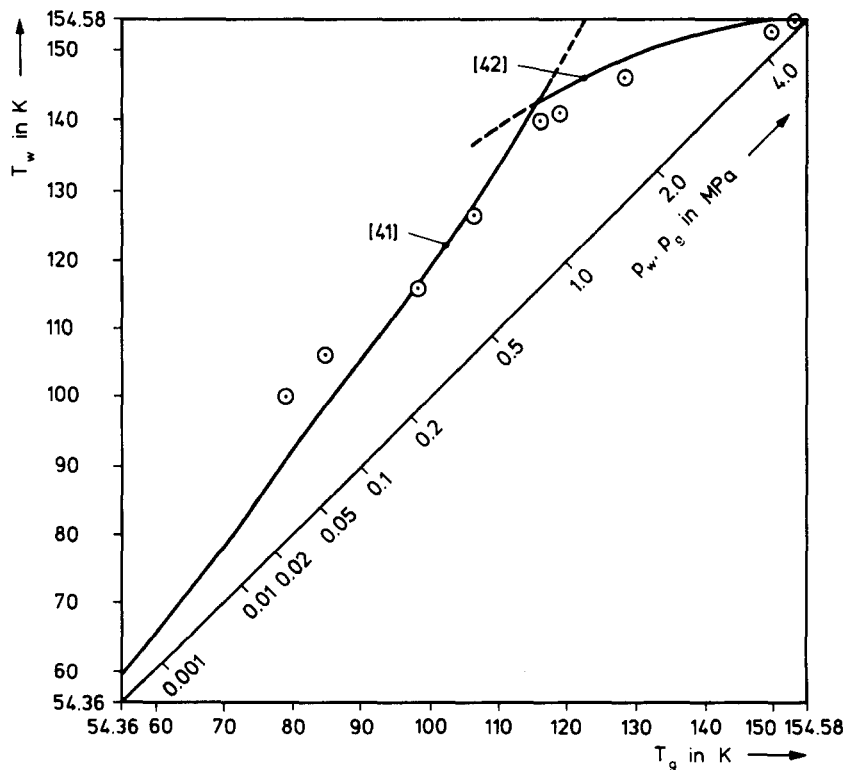

Figure 5. Peak nucleate boiling temperatures T_{DNB} of oxygen pool boiling by Kosky & Lyon (1968) compared with the present calculation.

The last lines of table 2 correspond to pressures where neither [41] nor [42] is applicable since our prediction of the DNB temperature has crossed the thermodynamic critical temperature, cf. upper right-hand corners of figures 4 and 5. Above the critical temperature no thermal properties for a liquid exist which could wet the heated surface. Thus we have assumed that the DNB temperature could be identical to the critical temperature in this range of system pressures. The results of table 2 emphasize this assumption within experimental scattering.

Besides the uncertainties of both pool boiling experiments and properties of state it could be that speed of sound data are completely unknown and [41] and [42] cannot be solved for the wall temperature. For the three measurements of R14 by Kosky & Lyon (1968) we used [44] for an idealized prediction of the vapour velocity but the liquid speed of sound has been extrapolated from correlations by Poole & Aziz (1972) and Aziz (1974) far outside the range of their validity. The results are plotted in figure 6 which covers a range of saturated states where data from Altumin et al. (1987) are known, i.e. no prediction is possible concerning DNB down to triple pressure. Figures 4, 5 and 6 might illustrate that the variety of fluids behave with very similar curves for DNB temperatures, i.e. the speed of sound of vapour limiting the heat transfer at low pressures with slightly increasing wall superheat. This condition changes to the limiting speed of sound of liquid at any attributed pressure where the wall superheat starts to decrease with increasing pressure until the wall temperature matches with the critical temperature and then the DNB temperature remains constant. This global tendency justifies the use of [44] at moderate pressure as carried out in section 6.1. In fact, figure 6 attributes verification to our theory for the single measurement at low pressure alone, since the high pressure speed of sound data have been estimated far away from the established range of applicability, but our theory is highly sensitive to incorrect speed of sound data at these high pressures.

Further problems arise when comparing the helium measurements, e.g. Lyon (1968), with our theory. This is due to the extremely low temperatures adjacent to absolute zero. From quantum mechanics we know that more than one speed of sound exists for a single phase and it is not always clear which of them is to be used within our model. Leaving out this long discussion we summarize that Schroeder-Richter (1991) has established the agreement of [42] with measurements down to about 3 K whereas the low pressure condition [41] predicts wall temperatures significantly lower than the measurements. Some experiments seem to be influenced by a liquid II to liquid I phase transition occurring at the λ-line ($T = 2.172$ K) in addition to boiling at the saturation line (three-phase boiling).

However, we jump to much higher temperatures and consider free convection boiling of liquid potassium. Properties including speed of sound of saturated vapour have been tabulated by Vargaftik (1975) in steps of 50 K. Thus we used data interpolations to enhance the precision of our analytical predictions. It should be mentioned that the Clausius–Clapeyron equation is to be calculated using variable molecular weight, since the boiling process is accompanied with chemical reactions from one-atomic to two-atomic molecules. Similar correction is necessary when using the ideal gas equation.

Kutateladze et al. (1973) report that the estimation of DNB temperatures for liquid metals is quite difficult as well, since very intense heat transfer is possible in single-phase flow. Sometimes the onset of nucleate boiling (ONB) promptly leads to dry patch formation (i.e. DNB) and in these

Table 2. Wall temperatures at the DNB of methane measured by Kosky & Lyon (1968) and compared with the present analytical prediction

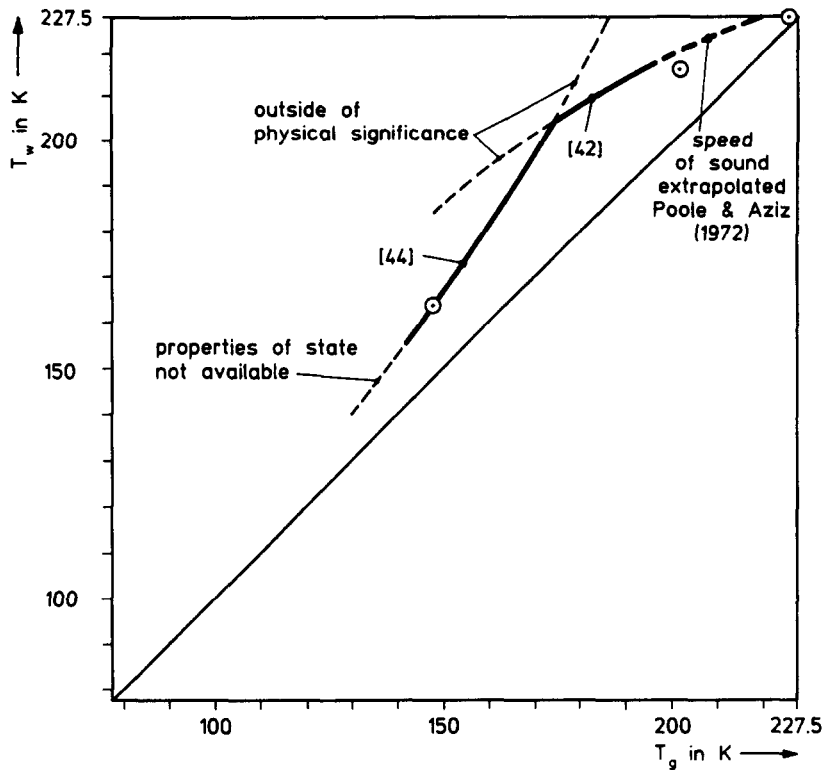| System pressure p_b (MPa)	Vapour temperature $T_s(p_g)$ (K)	Wall temperature at DNB, T_{DNB} (K)			
		Measured	[41]	[42]	Critical point
0.108	112.4	127.3	131.2		
0.108	112.4	133.1	131.2		
0.108	112.4	136.1	131.2		
1.641	160.7	177.3		185.0	
4.123	187.0	193.2			190.8
4.123	187.0	196.2			190.8
4.538	190.0	190.9			190.8
4.538	190.0	191.1			190.8

Figure 6. Peak nucleate boiling temperatures T_{DNB} of carbon tetrafluoride pool boiling by Kosky & Lyon (1968) compared with the present calculation.

cases the temperature of the heated wall corresponding to single-phase flow before ONB is higher than the wall temperature corresponding to DNB. Only temperatures at DNB conditions can be compared with [41]. On the other hand, Kutateladze *et al.* (1973) do not indicate which of their measurements started from nucleate boiling before the abrupt temperature rise was observed.

Therefore a rough comparison is given by adopting their figure (wall superheat versus pressure) and drawing a broken boundary which surrounds the whole of their measurements. Figure 7 shows our prediction [41] (heavy line) passing diagonally across the whole area of the considerably scattered data. This result merely indicates that we have predicted well the order of magnitude for the wall superheating at DNB of potassium. Nevertheless this was possible without any empirical coefficient adapted to these measurements. We have now predicted both a wall superheat of more than 100 K for potassium and a wall superheat of 26 K for caesium (cf. table 1). In summary our theory is verified when predicting the different orders of magnitude well. Considering now the large temperature range between helium boiling of about 3 K up to potassium boiling of about 1220 K we can no longer ignore the physical indication that our analytical model works well and the underlying hypothesis of an astonishing mechanical non-equilibrium seems to occur as well as the speed of sound.

However, most design problems for heat exchangers are connected with the boundary conditions of the second kind rather than the first kind as far as the heat transfer surface should be protected against a maximum heat flux. Boundaries of the first kind do not show that this situation leads to a crisis. Therefore an important question seems to be whether the DNB temperatures resulting from [41] or [42], respectively, could be inserted into [27] to estimate CHF.

7. CRITICAL HEAT FLUX

Numerous correlations already exist predicting the critical heat flux for a wide range of parameters. Thus, the present goal is not to stress our analysis up to a more general or more precise CHF estimation than is already known from recent methods at this first attempt. Instead we discuss
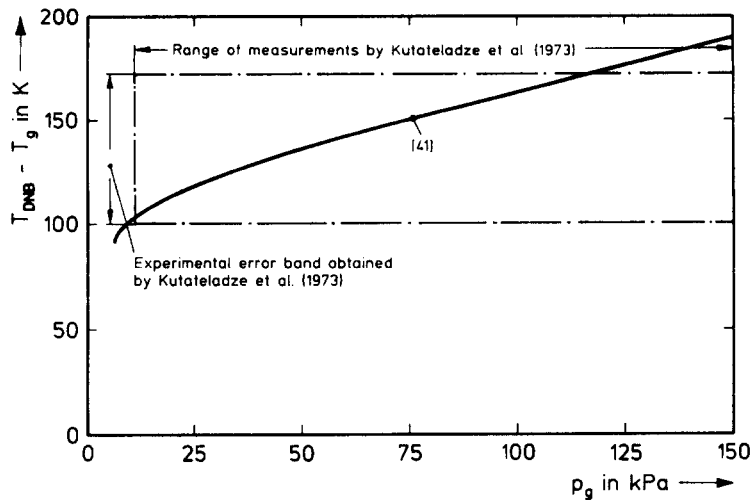
Figure 7. Critical wall superheat $(T_{DNB} - T_g)$ versus the system pressure p_b of potassium. Experimental error band by Kutateladze et al. (1973) compared with the present prediction.

some preliminary thoughts which could be valuable for a physically based prediction of CHF to be carried out by further studies.

It is well known that CHF is a multi-parameter problem. Besides flow parameters such as pressure, liquid temperature and mass flux, it depends on parameters of the flow channel such as heated length, diameter, material of the wall etc. and additionally on non-equilibrium effects such as distribution of heat flux which physically effects the CHF via the true void fraction governing the mechanisms DNB or dry out, respectively.

Since our model predicting DNB temperature exhibits dependence on pressure only, we restricted our preliminary analysis of CHF to the pressure effect, i.e. we only used the first term of [27] and inserted $T_w = T_{DNB}$ from [41] (at moderate pressure). The pressure dependence of coefficient B has been taken from Thom et al. (1965) within a constant. Results are shown in table 3.

To be sure that the other terms on the right-hand side of [27] do not violate our simplifications we furthermore restricted our analysis to measurements at small inlet subcoolings to the flow channel. Additionally, the mass flux effect of measurements could invalidate our comparison. Thus, we might prefer measurements at any arbitrarily selected but constant mass flux. On the other hand, this last statement has fixed the third of the flow parameters: pressure being varied, liquid sub-cooling being small, mass flux being arbitrarily fixed. Now we obtain an overdetermined goal considering that our model is valid for DNB alone. Our analysis has shown that the high pressure measurements tend to occur via dry out. Therefore mass flux has to be selected high enough as the CHF mechanism can be shifted to DNB again. Now the higher mass fluxes enhance the contribution of single-phase convection to the total heat transfer, i.e. the terms on the right-hand side of [27] affect the low pressure measurements.

Table 3. Comparison of heat fluxes calculated using [41] and [27] and measured by Johannsen & Weber (1988) during flow boiling of water through a temperature controlled tube. Data selected for lowest void fraction at each pressure and thus DNB being most probable (Schroeder-Richter 1991)

System pressure p_b (MPa)	Mass flux (kg/m² s)	Inlet subcooling (K)	q_{DNB} (MW/m²)	
			Measured	Predicted [41], [27]
0.11	100	5	2.2	2.0
0.25	100	5	2.9	2.8
0.40	200	5	3.8	3.5
0.70	200	5	5.0	5.0
1.00	200	6	5.7	5.7

Thus Schroeder-Richter (1991) obtained a compromise with respect to the mass flux when inspecting the most probable flow boiling measurements for selection of DNB as mentioned in section 6.2. The final result of this procedure is shown in table 3.

As mentioned above, the favourable agreement of a small number of selected data with our prediction should not lead to the conclusion that our attempt could readily be verified. Instead of this, it should encourage future work to correlate the phenomenological coefficients on the right-hand side of [27] as far as the sub-cooling effect is considered or to restore the dissipation Ψ', [11], into the analysis as far as the mass flux can be expressed as a driving force in a phenomenological equation similar to [25].

8. SUMMARY

It has been suggested that mechanical non-equilibrium in the cross section of a two-phase flow (boiling flow) should be taken into account in model development. This approach newly interprets the so-called superheated thermodynamic state of the wall layer. The results indicate that the state is not "superheated" but saturated at a higher pressure which can be explained as a thermomechanical effect.

The pressure difference can be calculated simply using the pressure of saturation corresponding to the known temperature at the heated surface. We have obtained astonishingly simple equations for heat transfer and DNB. It seems that DNB is physically governed by a sonic limit for the evaporation.

A consequence of this sonic limit is that wall temperatures are predicted. The analytical calculations were never restricted to special coolants, geometry, surface conditions or forced upflow. Consequently the model has been tested to predict DNB at different conditions (i.e. cryogenic liquids, water, liquid metals, pool boiling, forced convection) and has always been found to have favourable comparison with measurements, except for some data of boiling helium below 3 K. In turn, emphasis is given to the underlying assumption of a saturated state for the wetting liquid at the wall, by predicting DNB using a wide range of applicability.

Finally, a combination has been tested when predicting wall temperatures using our DNB model and then inserting the result into the heat transfer prediction. The results encourage this method to be followed when new CHF correlations are being developed. Of course, the present analysis is strongly restricted to boiling phenomena at low void fraction. Therefore, it would be desirable to try similar modelling of annular flow and dry-out mechanisms. The boiling curve at low void fraction has been completed by predicting transition to inverted annular flow (Huang et al. 1994) and the Leidenfrost temperature (Schroeder-Richter & Bartsch 1990) which furthermore emphasizes the hypothesis of a saturated wall layer at elevated pressure.

REFERENCES

ABHAT, A. 1984 High performance heat pipes for a latent heat thermal energy storage application. *Proc. 5th Int. Heat Pipe Conf.*, Vol. 1, pp. 321–327. Japan Technology & Economics Center, Tokyo.

ALTUMIN, V. V., GELLER, V.-Z., KREMENEVSKAYA, E. A., PERELSTEIN, I. I. & PETROV, E. K. 1987 *Thermophysical Properties of Freons, Methane Series, Part 2.* Hemisphere, Washington, DC.

AZIZ, R. A. 1974 Relative intermolar energy parameters for the freons from sound velocity data. *AIChE Jl* **20**, 817–818.

BARTSCH, G., BRITO, J. & SCHROEDER-RICHTER, D. 1990 Heat transfer coefficient of pool boiling within the heating zone of a two-phase closed thermosiphon. In *Fundamentals of Natural Convection* (Edited by ARPACI, V. S. & BAYAZITOUGLU, Y.), Vol. 140, pp. 99–104. ASME-HTD, New York.

BENNET, A. W., HEWITT, G. F., KEARSEY, H. A. & KEES, R. K. F. 1966 The wetting of hot surfaces by water in a steam environment at high pressure. AERE-R5146.

BERTHELOT, M. 1850 Sur quelques phenomenes de dilation forces des liquides. *Ann. Chim.* **30**, 332–337.

BRAUN, F. 1887 Untersuchung ueber die Loeslichkeit fester Koerper und die Vorgang der Loesung begleitenden Volum- und Energieaenderungen. *Z. Physik. Chem.* **1**, 259–272.

CELATA, G. P., CUMO, M., D'ANIBALE, F., FARELLO, G. E. & SETARO, T. 1986 Reassessment of forced convection heat transfer correlations for refrigerant 12. *Energia Nucl.* **3**, 1–14.

CHEN, J. C. 1963 A correlation for boiling heat transfer to saturated fluids in convective flow. ASME paper 63 HT 34, New York.

COOPER, M. G. 1989 Flow boiling—the 'apparently nucleate' regime. *Int. J. Heat Mass Transfer* **32**, 459–463.

DE GROOT, S. R. & MAZUR, P. 1963 *Non-equilibrium Thermodynamics.* North–Holland, Amsterdam.

ELSNER, N., FISCHER, S. & KLINGER, J. 1982 *Thermodynamische Stoffeigenschaften von Wasser.* VEB Grundstoffindustrie, Leipzig.

ELLIOTT, D. F. & ROSE, P. W. 1970 The quenching of heated surfaces by a film of water in a steam environment at pressure up to 53 bar. AEEW-M 976.

GROENEVELD, D. C. & SNOEK, C. W. 1986 A comprehensive examination of heat transfer correlations suitable for reactor safety analysis. In *Multiphase Science and Technology* (Edited by HEWITT, G. F., DELHAYE, J. M. & ZUBER, N.), Vol. 2, pp. 181–274. Hemisphere, Washington, DC.

HAHNE, E., SHEN, N. & SPINDLER, K. 1989 Fully developed nucleate boiling in upflow and downflow. *Int. J. Heat Mass Transfer* **32**, 1799–1808.

HEWITT, G. F. & HALL-TAYLOR, N. S. 1970 *Annular Two-phase Flow.* Pergamon Press, Oxford.

HOWARD, P. A. 1976 An experimental and analytical study of the sputtering phenomena. ANL-7641.

HUANG, X. C., BARTSCH, G. & SCHROEDER-RICHTER, D. 1994 Quenching experiments with a circular test section of medium thermal capacity under forced convection of water. *Int. J. Heat Mass Transfer.* **37**, 803–818.

HUNG, N. 1979 On the formulation of constitutive laws required to describe two-phase flow models. *Lett. Heat Mass Transfer* **6**, 513–518.

JANSEN, M. 1988 Ein Modell zur Berechnung des Dampfvolumenanteils und des Schlupfes in Zweiphasenstroemungen mit Zwangskonvektion im thermodynamischen Nichtgleichgewicht. Ph.D. thesis, TU Berlin.

JOHANNSEN, K. & WEBER, P. 1988 Experimental investigation of heat transfer in the transition region. Report, TU Berlin/EURATOM Contract No. 3013-86-07 EL ISP D.

KOSKY, P. G. & LYON, D. N. 1968 Pool boiling heat transfer to cryogenic liquids. *AIChE Jl* **14**, 372–387.

KUTATELADZE, S. S., MOSKVICHEVA, V. N., BOBROVICH, G. I., MAMONTOVA, N. N. & AVKSENTYUK, B. P. 1973 Some peculiarities of heat transfer crisis in alkali metals boiling under free convection. *Int. J. Heat Mass Transfer* **16**, 705–713.

LE CHATELIER, H. 1888 Recherches experimentales et theoretiques sur les equilibres chemiques. *Ann. Mines* **13**, 157–382.

LEIDENFROST, J. G. 1756 De aquae nonnullis qualitatibus tractus. Duisburg—WARES, C. (translation of Ch. 15–35) 1966 On the fixation of water on diverse fire. *Int. J. Heat Mass Transfer* **9**, 1153–1166.

LYON, D. N. 1968 Pool boiling of cryogenic liquids. *Adv. Cryogen. Heat Transfer, Chem. Engng Prog. Symp. Ser.* **64**, 82–92.

MERTE, H. & CLARK, S. A. 1964 Boiling heat transfer with cryogenic fluids at standard, fractional and near zero gravity. *J. Heat Transfer* **86**, 351–359.

MEYER, J. 1911 Zur Kenntnis des negativen Druckes in Fluessigkeiten. *Z. Elektrochem.* **17**, 743–745.

MICHEL, H. 1984 Statistische Methode zur Bestimmung des Waermetransportes zwischen Heizflaeche, Dampfblase und Fluessigkeit und des Dampfvolumenanteiles beim unterkuehlten Stroemungssieden. Ph.D. thesis, TU Berlin.

MITROVIC, J. 1983 Das Abreissen von Dampfblasen an festen Heizflaechen. *Int. J. Heat Mass Transfer* **26**, 955–963.

MUELLER, I. 1985 *Thermodynamics.* Pitman, Boston, MA.

MUSCHIK, W. & MUELLER, W. H. 1983 Bilanzgleichungen offener mehrkomponentiger Systeme, part I and II. *J. Non-equilibrium Thermodyn.* **8**, 29–66.

NEGISHI, K., KANEKO, K.-I. & KUSUMOTO, F. 1987 Analysis of pulsation in two-phase thermosiphons. *Proc. 6th Int. Heat Pipe Conf.*, Vol. 2, pp. 588–592, CEA, Grenoble, France.

NGUYEN-CHI, H. & GROLL, M. 1982 Entrainment or flooding limit in a closed two-phase thermosiphon. In *Advances in Heat Pipe Technology* (Edited by REAY, D. A.), pp. 147–162. Pergamon Press, Oxford.

POOLE, G. R. & AZIZ, R. A. 1972 Sound velocity in liquid C Cl$_2$ F$_2$ and the law of corresponding states. *AIChE Jl* **18**, 430–432.

PRIGOGINE, I. 1947 *Etude Thermodynamique des Phenomenes Irreversibles.* Dunod, Paris.

RABINOVICH, V. A., VASSERMAN, A. A., NEDUSTUP, V. I. & VEKSLER, L. S. 1987 *Thermophysical Properties of Neon, Argon, Krypton and Xenon.* Hemisphere, Washington, DC.

SCHAAFS, W. 1967 *Molecular Acoustics, Landolt–Boernstein, Numerical Data and Functional Relationships in Science and Technology*, New Series, Group II, Vol. 5, p. 8.

SCHMIDT, E. 1982 Properties of water and superheated steam in SI-units, 0–800°C, 0–1000 bar (Edited by GRIGULL, U.). Springer, Berlin.

SCHROEDER-RICHTER, D. 1991 *Ein analytischer Beitrag zur Anwendung der Thermodynamik irreversibler Prozesse auf Siedephaenomene.* VDI, Duesseldorf.

SCHROEDER-RICHTER, D. & BARTSCH, G. 1990 The Leidenfrost phenomenon caused by a thermo-mechanical effect of transition boiling: a revisited problem of non-equilibrium thermodynamics. In *Fundamentals of Phase Change: Boiling and Condensation* (Edited by WHITE, L. C. & AVEDISIAN, C. T.), Vol. 136, pp. 13–20. ASME-HTD, New York.

SHIRES, G. L., PICKERING, A. R. & BLACKER, P. T. 1964 Film cooling of vertical fuel rods. AEEW-R 343.

SPIEGLER, P., HOPENFELD, J., SILBERBERG, M., BUMPUS, C. F. JR. & NORMAN, A. 1963 Onset of stable film boiling and the foam limit. *Int. J. Heat Mass Transfer* **6**, 987–989.

SYCHEV, V. V., VASSERMAN, A. A., KOZLOV, A. D., SPIRIDONOV, G. A. & TSYMARNY, V. A. 1987a *Thermodynamic Properties of Nitrogen.* Hemisphere, Washington, DC.

SYCHEV, V. V., VASSERMAN, A. A., KOZLOV, A. D., SPIRIDONOV, G. A. & TSYMARNY, V. A. 1987b *Thermodynamic Properties of Oxygen.* Hemisphere, Washington, DC.

SYCHEV, V. V., VASSERMAN, A. A., ZAGORUCHENKO, V. A., KOZLOV, A. D., SPIRIDONOV, G. A. & TSYMARNY, V. A. 1987c *Thermodynamic Properties of Methane.* Hemisphere, Washington, DC.

THOM, J. R. S., WALKER, M. W., FALLON, T. A. & REISING, G. F. S. 1965 Boiling in subcooled water during flow in tubes and annuli. *Proc. Inst. Mechanical Engineers*, 3C180, pp. 226–246.

TONG, L. S. & WEISMAN, J. 1979 *Thermal Analysis of Pressurized Water Reactors*, 2nd edn, pp. 285–288. ANS, IL.

ULRYCH, G. 1976 Stroemungsvorgaenge in Kernreaktoren mit unterkuehltem Sieden. Ph.D. thesis, TU Braunschweig.

VARGAFTIK, N. B. 1975 *Tables on the Thermophysical Properties of Liquids and Gases.* Hemisphere, Washington, DC.

WEBER, P. 1990 *Experimentelle Untersuchungen zur Siedekrise und zum Uebergangssieden von stroemendem Wasser unter erhoehtem Druck.* VDI, Duesseldorf.

ZUBER, N. 1958 On the stability of boiling heat transfer. *Trans. ASME* **80**, 711–720.